Metal Coordination Sphere Deformation Induced Highly Stokes-Shifted, Ultra Broadband Emission in 2D Hybrid Lead-Bromide Perovskites and Investigation of Its Origin

Metal Coordination Sphere Deformation Induced Highly Stokes-Shifted, Ultra Broadband Emission in 2D Hybrid Lead-Bromide Perovskites and Investigation of Its Origin

Benny Febriansyah[+], Tetiana Borzda[+], Daniele Cortecchia, Stefanie Neutzner, Giulia Folpini, Teck Ming Koh, Yongxin Li, Nripan Mathews, Annamaria Petrozza, and Jason England**

Abstract: Published studies of layered (2D) (100)-oriented hybrid lead-bromide perovskites evidence a correlation between increased inter-octahedral (Pb-Br-Pb) distortions and the appearance of broadband white light emission. However, the impact of distortions within their constituent $[PbBr_6]^{4-}$ octahedra has yet to be assessed. Herein, we report two new (100)-oriented 2D Pb-Br perovskites, whose struc- tures display unusually high intra-octahedral distortions, whilst retaining minimal inter-octahedral distortions. Using a combi- nation of temperature-dependent, power-dependent and time- resolved photoluminescence spectroscopic measurements, we show that increased intra-octahedral distortion induces exciton localization processes and leads to formation of multiple photoinduced emissive colour centres. Ultimately, this leads to highly Stokes-shifted, ultrabroad white light emission at room temperature.

Two-dimensional (2D) hybrid Pb-Br perovskites that exhibit broadband emission, upon near-ultraviolet (UV) excitation, are an intensely studied class of materials.[1,2] Interest in them originates from their potential as single-source down-converting white-light-emitting phosphors, displaying good color rendition and stable emission color.[3,4] Furthermore, they can be deposited on large surface area substrates from solution, at relatively low temperatures, and without the need of additives, which makes them attractive in terms of cost and ease of fabrication.[5] Recent works have allowed compilation of a library of these compounds, leading to the development of further broadband emitting metal halides along with an understanding of how these properties can be induced.[1,2,6–11]

Despite this surge in the synthesis of new Pb-Br perovskites, the photophysical origins of the observed photoluminescence broadening are still uncertain. The strong coulombic and dielectric confinement typical of 2D perovskites leads to the formation of tightly bound excitons that can interact with the polar perovskite lattice. Several studies have highlighted the photoinduced formation of self-trapped excitons, which can be described as small polarons, where the excess charge is spatially confined within one crystal unit cell, thereby causing local structural reorganization of the inter-atomic distances. Mechanisms involving formation of several different species have been proposed as the key pathway leading to ultra-broadband, highly Stokes shifted emission.[5,12] This includes self-trapped electrons (STEL, Pb_2^{3+}), self-trapped holes (STH, Pb^{3+} and X_2^{-}), and Jahn–Teller and V_k self-trapped excitons, involving localization of charges at specific crystal sites by their own lattice distortion fields.[2,13–18] Most evidence for these hypotheses comes from theoretical works, and rigorous experimental support is lacking.[18–21] Alternatively, it has been suggested that permanent color centers (e.g., positive and negative ion vacancies, and atoms in interstitial sites) play a key role in mediating the observed trapping and luminescence processes.[22,23]

Regardless, it is widely accepted that the structural properties of a perovskite, including dimensionality, control the energetic landscape and defectivity, and thereby directly affect emission energy and bandwidth.[5,9,18,24,25] This has important synthetic implications, since the desired level and type of structural distortion can be tailored by incorporation of carefully selected organic cations. Correspondingly, several recent reports have attempted to establish correlations between structural and optical properties of two-dimensional (2D) perovskites.[8–10]

Structurally, 2D Pb-halide perovskites can be viewed as being derived from their 3D counterparts by slicing the inorganic lattice of the latter along either the (100), (110), or (111) crystallographic planes.[26,27] Early on, broadband emis-

[*] B. Febriansyah,[+] Dr. Y. Li, Prof. J. England
Division of Chemistry and Biological Chemistry, School of Physical and Mathematical Sciences, Nanyang Technological University
21 Nanyang Link, Singapore 637371 (Singapore)
E-mail: jengland@ntu.edu.sg
Dr. T. Borzda,[+] Dr. D. Cortecchia, Dr. S. Neutzner, Dr. G. Folpini, Prof. A. Petrozza
Center for Nano Science and Technology @Polimi
Istituto Italiano di Tecnologia
8 via Giovanni Pascoli 70/3, 20133 Milan (Italy)
E-mail: annamaria.petrozza@iit.it
B. Febriansyah,[+] Dr. T. M. Koh, Prof. N. Mathews
Energy Research Institute at Nanyang Technological University (ERI@N)
Research Techno Plaza, X-Frontier Block Level 5, 50 Nanyang Drive, Singapore 637553 (Singapore)
B. Febriansyah[+]
Interdiscipinary Graduate School (IGS)
50 Nanyang Avenue, Singapore 639798 (Singapore)
Prof. N. Mathews
School of Materials Science and Engineering
Nanyang Technological University
50 Nanyang Avenue, Singapore 639798 (Singapore)
[+] These authors contributed equally to this work.

sion was linked to Pb-Br perovskites bearing comparatively rare corrugated (110)-oriented structures.[1,2,7,8,11,19] Later, more common (100) Pb-Br variants, which typically emit narrow free-excitonic (FE) PL in the blue or near-UV region, were also found to exhibit similar broad PL features, albeit with a strong dependence on temperature. In particular, Smith et al. suggested a correlation between greater out-of- plane inter-octahedral distortions of the crystal lattice in (100) Pb-Br perovskites and increased relative intensity of broad- band emission.[9] Subsequent reports by Neogi,[10] Wang,[3] and Hu[4] further supported this conclusion. In contrast to the high out-of-plane tilt angles, the $PbBr_6$ units in all of these reports retain a "close-to-ideal" octahedral coordination geometry.[3,4,10]

The influence of structural distortion within the coordination sphere of the lead ions (i.e. "intra-octahedral distortion"), rather than between Pb-Br octahedra ("inter-octahedral distortion"), upon broadband emission has not been investigated. This is largely due to the absence of materials displaying the latter without the former. In response, we synthesized bromoplumbates of the ethylammonium-appended cyclic dications 1 and 2 (Figure 1), which template 2D Pb-I perovskites displaying large intra-octahedral distortions.[29] X-ray crystallographic characterization confirmed that the desired 2D perovskites 1[$PbBr_4$] and 2[$PbBr_4$] (Figure 2, Table S1) were obtained, and the purity of the bulk materials was established using powder X-ray diffraction (Figure S1).

Both 1[$PbBr_4$] and 2[$PbBr_4$] feature a conventional (100) structure, with single-layer-thick corner-shared octahedral $[PbBr_6]^{4-}$ units separated by monolayers of dications 1 or 2. The compact nature of the dications leads to very small distances between the inorganic layers of ca. 4.169 and 4.069 Å, respectively. The degree of intra-octahedral structural distortion of the inorganic layers was assessed quantitatively by calculation of octahedral elongation (l_{oct}), octahedral angle variance (s^2_{oct}), and octahedral bond-length distortion (D_{oct}) parameters, which are explained in the supporting information and elsewhere.[8,24,28] For all of the parameters, larger values correspond to greater distortion. The intra-octahedral distortions exhibited by 1[$PbBr_4$] and 2[$PbBr_4$] are large compared with other (100) perovskites (Tables 1 and S2). Instead, they are of a similar order of magnitude to those reported for (110) perovskites (Table S3). As a consequence of lattice contraction, the high degree of intra-octahedral distortion of the inorganic lattice becomes more obvious at low temperatures (100 K). Under these conditions, 2 was found to enforce much more severe octahedral elongation and angle variance than 1 (Figure S2, Table S4). Differences between the interactions of 1 and 2 and their respective bromoplumbate lattices manifest in their Raman spectra (Figure S3 and accompanying discussion).

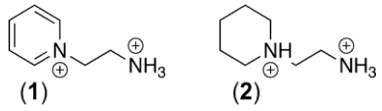

Figure 1. The organic dications, 1 and 2, used in this study.

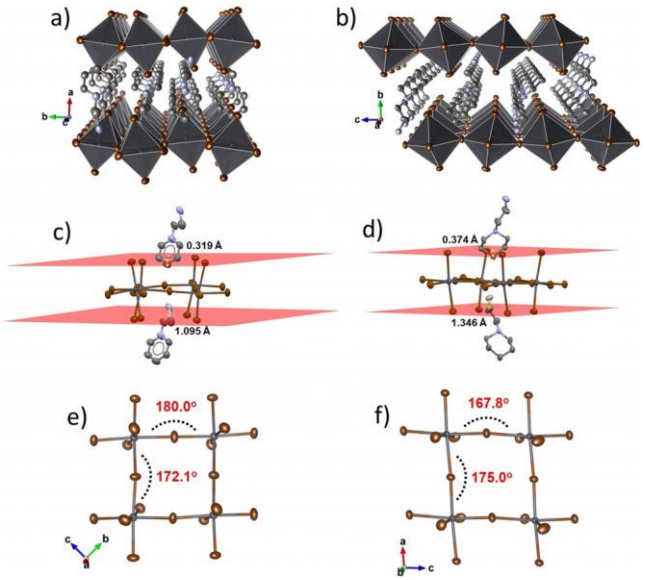

Figure 2. Room temperature X-ray crystal structures of a) 1[$PbBr_4$] and b) 2[$PbBr_4$]. Penetration of the organic dications into the "bay regions" of the 2D perovskites, built from four nearest neighbor $[PbBr_6]^{4-}$ octahedra, are depicted in c) 1[$PbBr_4$] and d) 2[$PbBr_4$]. The approximate depth of penetration (Å) of the ethylammonium and heterocyclic groups are given in the Figure (dotted orange lines). "Top views" of e) 1[$PbBr_4$] and f) 2[$PbBr_4$] are presented, with their respective crystallographic axes and Pb-(m-Br)-Pb bond angles. Black, brown, grey, and blue spheroids represent Pb, Br, C, and N atoms, respectively. H atoms are omitted for clarity. Ellipsoids are shown at 50 % probability.

Table 1: Summary of distortion parameters for 1[$PbBr_4$], 2[$PbBr_4$], and selected 2D Pb-Br perovskites.[a]

Compound	l_{oct}[b]	s^2_{oct}[c]	D_{oct} [$\times 10^{-4}$][d]	D_{tilt} [8][e]	D_{out} [8][f]	D_{in} [8][g]
1[$PbBr_4$]	1.0104	30.09	13.655	7.9	6.0	5.1
2[$PbBr_4$]	1.0109	33.99	9.460	12.2	10.5	6.2
DMABA[$PbBr_4$][8]	1.0094	32.64	4.300	17.1	16.7	3.9
AEA[$PbBr_4$][9]	1.0060	20.72	0.852	35.7	22.4	28.5
CyDMA[$PbBr_4$][10]	1.0016	5.09	0.855	32.3	23.2	23.0
MPenDA[$PbBr_4$][9]	1.0007	2.58	0.004	32.6	17.9	27.7
$(PEA)_2$[$PbBr_4$][29]	1.0056	16.35	9.770	29.2	10.4	27.9
$(BA)_2$[$PbBr_4$][9]	1.0027	9.43	0.067	25.2	2.8	25.0

[a] See SI for the structures of the organic cations. With the exception of $(PEA)_2$[$PbBr_4$] and $(BA)_2$[$PbBr_4$], all are broadband emitters at room temperature. [b] Octahedral elongation. [c] Octahedral angle variance. [d] Octahedral bond-length distortion. [e] $D_{tilt} = 180 - q_{tilt}$. [f] $D_{out} = 180 - q_{out}$. [g] $D_{in} = 180 - q_{in}$. q_{tilt}, q_{in}, and q_{out} are Pb-(m-Br)-Pb angle, and in-plane and out-of-plane projections of the Pb-(m-Br)-Pb angle, respectively.

The large intra-octahedral distortions in our compounds can be attributed to the inherently asymmetric environment of their constituent $[PbBr_6]^{4-}$ octahedra.[30] More specifically, the organic dications within a monolayer alternate in terms of their orientation, with either their cyclic heads or ethylammonium tails pointing into the "bay regions"[31,32] formed by the terminal bromide ligands of four nearest neighbour Pb-Br octahedra (Figures 2 c,d). In addition, the two "bay regions" on opposing faces of the 2D inorganic layers host

different ends (heads or tails) of the dications. This asymmetry is exacerbated by the large difference between penetration of the heads and tails of the dications into the "bay regions" of the perovskites. Detailed discussion of this is provided, following Figure S2, in the Supporting Information.

Conversely, 1[$PbBr_4$] and 2[$PbBr_4$] exhibit minimal inter-octahedral distortions, with those of the latter being slightly higher than the former (Table 1). This is evident in their Pb-(m-Br)-Pb bond angles, which are as high as 180 and 175**8**, respectively (q_{tilt}; Figures 2 e,f). As a frame of reference, typical Pb-(m-Br)-Pb bond angles reported for (100) 2D Pb-Br perovskites range between 144 and 153**8**.[9,10,29,33] More thorough quantification of the inter-octahedral distortions is provided by their respective in-plane (D_{in}) and out-of-plane (D_{out}) distortion parameters (see Table 1 and ref. [21]), which can be calculated using the methodology employed in ref. [21]. Small values of 5.1 and 6.0**8** were obtained for 1[$PbBr_4$] and 6.2 and 10.5**8** for 2[$PbBr_4$] (Table 1). In contrast, inter-octahedral distortion angles of reported white light emitting (100) 2D bromoplumbates exceed 15**8**.[3,4,9,10] Importantly, the minimal inter-octahedral distortions in the two compounds are retained even at low temperature (100 K; Figure S2 and Table S4).

The small inter-octahedral distortions observed for 1-[$PbBr_4$] and 2[$PbBr_4$], relative to templating cations containing only primary ammonium groups, are likely due to the relatively diffuse, sterically hindered positive charges of the cyclic rings present in 1 and 2. By comparison, primary ammonium groups have highly localized and accessible positive charges. One would anticipate that the latter cations would exert a greater driving force for bringing the negatively charged lead-halide octahedra into close proximity with them, thereby distorting the inorganic lattice. This would manifest as a compression of the Pb-(m-X)-Pb bond angles (in-plane and/or out-of-plane) between neighboring octahedra. The reduced quantities of primary ammonium cations in our materials relative to conventional perovskites, therefore, leads to reduced inter-octahedral distortions.[30,34]

In essence, dications 1 and 2 both template (100) 2D Pb-Br perovskites that exhibit large intra-octahedral distortions of the inorganic lattice, but without enforcing appreciable inter-octahedral tilting. This has a significant impact upon the single crystal optical properties of 1[$PbBr_4$] and 2[$PbBr_4$]. Figures 3 a and b show the Kubelka–Munk transformed UV-vis reflectance (R) data measured using ground crystals. The excitonic peak of the layered perovskites appears as a sharp band located at 434 and 422 nm in 1[$PbBr_4$] and 2[$PbBr_4$], respectively. The absorption blue-shift of 2[$PbBr_4$] correlates well with its slightly smaller average Pb-(m-Br)-Pb angles relative to 1[$PbBr_4$]. As previously stated,[30,35] this greater deviation from linearity results in poorer orbital overlap (Pb-6s and Br-4p orbitals) and causes widening of the band-gap.

The higher levels of intra- and inter-octahedral distortion in the structure of 2[$PbBr_4$], relative to 1[$PbBr_4$], results in striking differences in the steady-state photoluminescence (PL) properties of these two materials. At room temperature, the emission of the less-distorted compound 1[$PbBr_4$] features a predominant narrowband, blue emission ranging from 430 to 500 nm, with a broad and unstructured tail. The high

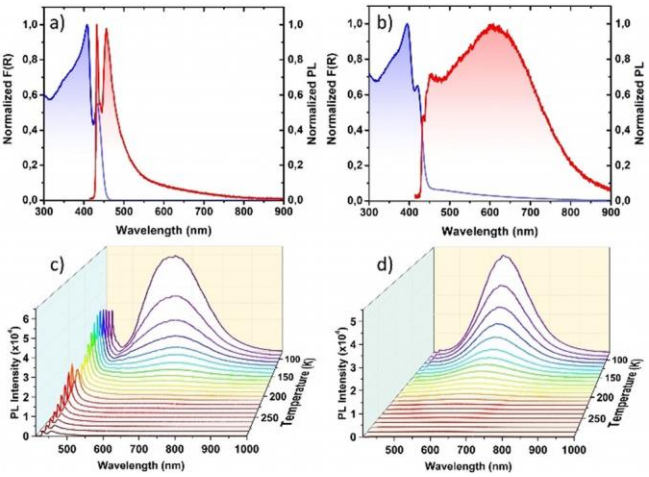

Figure 3. Absorption (blue line) and luminescence (red line) spectra of a) 1[$PbBr_4$] and b) 2[$PbBr_4$], at room temperature. Temperature-dependent photoluminescence of c) 1[$PbBr_4$] and d) 2[$PbBr_4$]. PL spectra were recorded for single crystals, using I_{ex} of 405 nm.

energy emission shows a double-peaked structure that results from the self-absorption of the excitonic emission, which is particularly strong in single crystals of compounds that exhibit a very small Stokes-shift.[36] This is confirmed by time resolved PL measurements (see below) and the fact that PL spectra measured on thin films, where the influence of luminescence self-absorption is greatly reduced, show a single-peaked excitonic emission (Figure S4).

On the other hand, the more distorted compound 2-[$PbBr_4$] has an ultrabroad (full width at half maximum (FWHM) = 292 nm or 1.1 eV), heavily Stokes shifted (203 nm) emission peak centred at 607 nm, which partially overlaps with the free excitonic emission peak at 452 nm. Similar optical properties are retained when this perovskite is spin-coated as a thin film (Figure S4), indicating that the emission is morphology-independent. This broadband emission corresponds to nearly pure white-light, with a correlated colour temperature (CCT) = 4088, Commission Internationale de l'Eclairage (CIE) chromaticity coordinate (0.38; 0.38) and colour rendering index (CRI) = 96 (Figure S5). This CRI value is higher than that of fluorescent light sources (about 65) and surpasses the values reported for other 2D white-light emitting perovskites.[5,37]

As is typically observed in other layered Pb-Br perovskites,[5] broadband emission becomes dominant in both 1[$PbBr_4$] and 2[$PbBr_4$] at low temperatures, increasing in intensity by about two orders of magnitude upon moving from 298 to 77 K (Figures 3 c, d and Figure S6). This increase is accompanied by narrowing of the band and a redshift of the peak in the temperature (T) range 298 to ≈150 K, followed by a blue-shift upon decreasing $T < 150$ K (Figure S7). The dependence of the integrated PL intensity upon temperature follows Arrhenius-type behaviour, with at least two non-radiative thermally activated channels being present. The dominant channels are E_a = 122 meV for 1[$PbBr_4$] and E_a = 140 meV for 2[$PbBr_4$], respectively (see Table S6 and Fig- ure S8). The less distorted structure of 1[$PbBr_4$] exhibits lower

de-trapping energies, which result in a faster quenching of the broadband PL with temperature. The presence of multiple thermally activated channels suggests that radiative decay involves a distribution of sub-band-gap states stemming from exciton trapping at different sites of the perovskite lattice, ultimately leading to ultrabroad PL.

Figure 4 shows power-dependent PL measurements performed at 77 K. The integrated spectra, plotted in double-logarithmic scale, exhibit power law dependence $I = P^K$, where I is PL intensity and P is excitation power. As expected for an excitonic transition, the intensity of the excitonic emission peak in 1[$PbBr_4$], at 430 nm, increases linearly with increasing excitation power and, thus, $K \approx 1$ (Figures 4 a and S9).[38] On the other hand, a sublinear trend is observed for the broadband component (460–900 nm) in both 1[$PbBr_4$] and 2[$PbBr_4$], with K = 0.89 0.01 and 0.95 0.01, respectively (Figure 4 b). A similar trend was also previously observed for the broadband emission of $Cs_3Sb_2I_9$.[39] However, such behaviour is contrary to the majority of similar broadband emitting perovskites. Therein PL intensity exhibits a linear dependence upon excitation density and does not show saturation behavior, which has been interpreted as a signature trait of self-trapped exciton formation.[5]

PL excitation-power dependence in semiconductors with $K < 1$ is characteristic of emission of excitons bound to donor–acceptor pairs (DAP recombination).[38] It has been suggested that the various defects that hybrid perovskites are prone to,[40,41] owing to their soft metal halide lattice, can offer sites for DAP mediated luminescence.[42] However, strong electron-phonon interactions characteristic of 2D perovskites have also been shown to promote exciton trapping at specific sites of the crystal lattice, induced by their own lattice distortion fields. Such localization effects pose additional restrictions upon the rate of radiative recombination. These are not taken into account in the derivation of the power law model and might render it inaccurate for the analysis of self-trapped exciton emission.[38,39] In an effort to differentiate between these possibilities, we investigated the materials charge carrier relaxation dynamics via temperature-dependent time-resolved PL measurements.

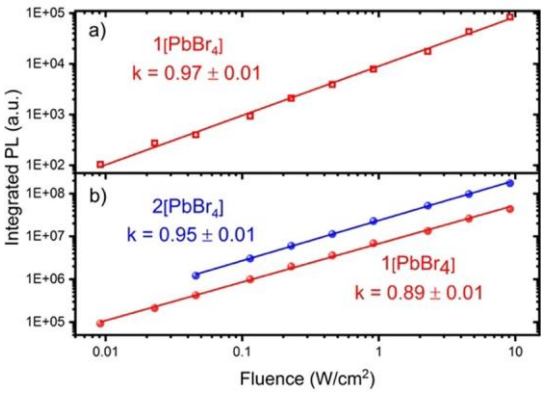

Figure 4. Integrated PL intensity, at 77 K, as function of excitation fluence. a) 1[$PbBr_4$] with an integration range of 428–435 nm; b) broadband emission of 1[$PbBr_4$] (red line) and 2[$PbBr_4$] (blue line) with integration ranges of 460–900 nm. PL spectra were recorded for single crystals, using I_{ex} of 405 nm.

The measured time-resolved PL spectra are presented in Figure 5. We fit our time-resolved PL data at both 298 and 77 K to a stretched exponential function (see SI for details), in which the effective decay time is stretched by a factor, b, referred to as the lifetime distribution parameter. At 298 K, excitonic emission of 1[$PbBr_4$] almost completely decays within 30 ps (Figures 5 a and S10), whereas the broadband emission of 2[$PbBr_4$] (integrated over the range 450–750 nm) undergoes a slower decay, with an effective lifetime (t_{eff}) of 120 ps and b = 0.67 (Figure 5 a). At 77 K, the t_{eff} of the broadband emission of 2[$PbBr_4$] increases to 19 ns and the decay becomes close to monoexponential (b = 0.93) (Figure 5 b). In contrast, the low energy broadband emission of 1[$PbBr_4$] shows a stretched-exponential decay with t_{eff} = 2.24 ns and a low b value of 0.25.

Decay that is well described using a stretched-exponent is indicative of PL derived from a distribution of decay rates. The latter is suggestive of spatial inhomogeneity in the distribution of trap states. From the decreasing FWHM of the PL band of 2[$PbBr_4$] with decreasing temperature, it can be inferred that there is a broad distribution of trap states at ambient temperatures, presumably due to the thermal accessing of other discrete emissive states in the lattice, which transforms to a much narrower distribution at 77 K. This is consistent with the observed almost monoexponential decay of its broadband emission at low temperature. As such, the slower lifetime signature and larger lifetime distribution of 2[$PbBr_4$] at low temperature, compared with 1[$PbBr_4$], can be ascribed to its more distorted structure which provides different luminescent color centers, leading to distinct recom- bination dynamics of the material.

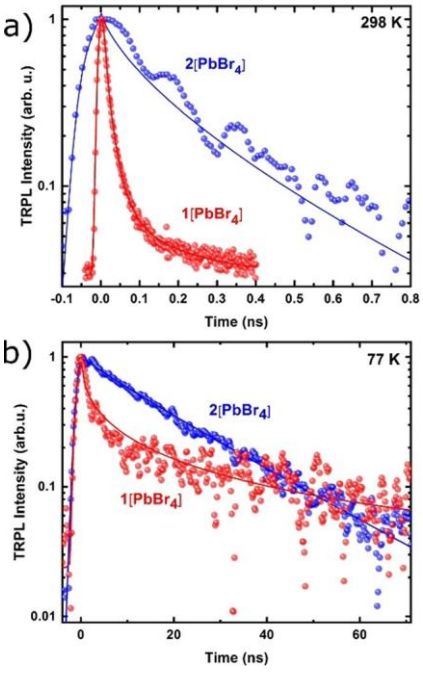

Figure 5. Time-resolved PL spectra of 1[$PbBr_4$] and 2[$PbBr_4$]. a) Excitonic emission of 1[$PbBr_4$] (in the range 420–435 nm) and broadband emission of 2[$PbBr_4$] (in the range 450–750 nm) at 298 K; b) broadband emission of 1[$PbBr_4$] and 2[$PbBr_4$] (in the range 470–750 nm) at 77 K. Data was recorded for single crystals, using I_{ex} of 368 nm.

In summary, we employed the ditopic dications 1 and 2 to template the (100)-oriented 2D perovskites 1[$PbBr_4$] and 2[$PbBr_4$]. Uniquely, their bromoplumbate layers feature high levels of intra-octahedral distortion, but only minimal inter-octahedral tilting. This was rationalized in terms of the supramolecular interactions between the inorganic lattice and highly asymmetric templating cations, and enabled us to study the impact of distortion within the $[PbBr_6]^{4-}$ octahedra upon the perovskite optical properties. Highly Stokes-shifted, ultra-broadband white light emission is observed in both compounds at low temperature (77 K), but it is retained at room temperature only in the case of the more distorted compound 2[$PbBr_4$] (CRI = 96 and FWHM = 292 nm). To date, room temperature emissive behaviour in (100)-oriented 2D Pb-Br perovskites has been observed exclusively for structures displaying very large inter-octahedral distortions. Based upon power-dependent, temperature-dependent, and time-resolved PL studies, we conclude that increased intra-octahedral distortion induces exciton localization processes and leads to formation of multiple photoinduced emissive colour centres. Given that large-scale intra-octahedral distortions can be induced by judicious selection of dications containing two sterically divergent ammonium ions, it is clear that this work offers a new avenue by which ultra-broadband white light emission can be induced in Pb-Br perovskites. Future work might involve optimization of optoelectronic performance by fine-tuning of the intra-octahedral distortions (via changes in the structure of the templating cation) or by alloying with a small organic cation, such as methylammonium, to provide 2D multilayer ($n > 1$) Pb-Br perovskites.

CCDC 1915485, 1915486, 1966108 and 1966109 contain the supplementary crystallographic data for this paper. These data can be obtained free of charge from The Cambridge Crystallographic Data Centre.

Acknowledgements

J.E. thanks NTU for funding (M4081442). B.F., T.M.K. and N.M. would like to acknowledge the funding from the Singapore National Research Foundation through the Intra-CREATE Collaborative Grant (NRF2018-ITC001-001), Office of Naval Research Global (ONRG-NICOP-N62909- 17-1-2155), and the Competitive Research Program: NRF-CRP14-2014-03. A.P. and T.B. have been funded by the ERCCoG project SOPHY under grant agreement N 771528.

Conflict of interest

The authors declare no conflict of interest.

Keywords: crystal engineering · intra-octahedral distortion · lead-bromide perovskites · photophysics · white-light emission

[1] E. R. Dohner, E. T. Hoke, H. I. Karunadasa, *J. Am. Chem. Soc.* 2014, *136*, 1718 – 1721.
[2] E. R. Dohner, A. Jaffe, L. R. Bradshaw, H. I. Karunadasa, *J. Am. Chem. Soc.* 2014, *136*, 13154 – 13157.
[3] S. Wang, Y. Yao, J. Kong, S. Zhao, Z. Sun, Z. Wu, L. Li, J. Luo, *Chem. Commun.* 2018, *54*, 4053 – 4056.
[4] H. Hu, S. A. Morris, X. Qiao, D. Zhao, T. Salim, B. Chen, E. E. M. Chia, Y. M. Lam, *J. Mater. Chem. C* 2018, *6*, 10301 – 10307.
[5] M. D. Smith, H. I. Karunadasa, *Acc. Chem. Res.* 2018, *51*, 619 – 627.
[6] Y. Y. Li, C. K. Lin, G. L. Zheng, Z. Y. Cheng, H. You, W. D. Wang, J. Lin, *Chem. Mater.* 2006, *18*, 3463 – 3469.
[7] Y. Li, G. Zheng, J. Lin, *Eur. J. Inorg. Chem.* 2008, 1689 – 1692.
[8] L. Mao, Y. Wu, C. C. Stoumpos, M. R. Wasielewski, M. G. Kanatzidis, *J. Am. Chem. Soc.* 2017, *139*, 5210 – 5215.
[9] M. D. Smith, A. Jaffe, E. R. Dohner, A. M. Lindenberg, H. I. Karunadasa, *Chem. Sci.* 2017, *8*, 4497 – 4504.
[10] I. Neogi, A. Bruno, D. Bahulayan, T. W. Goh, B. Ghosh, R. Ganguly, D. Cortecchia, T. C. Sum, C. Soci, N. Mathews, S. G. Mhaisalkar, *ChemSusChem* 2017, *10*, 3765 – 3772.
[11] B. Febriansyah, D. Giovanni, S. Ramesh, T. M. Koh, Y. Li, T. C. Sum, N. Mathews, J. J. England, *J. Mater. Chem. C* 2020, *8*, 889 – 893.
[12] R. T. Williams, K. S. Song, *J. Phys. Chem. Solids* 1990, *51*, 679 – 716.
[13] T. Hu, M. D. Smith, E. R. Dohner, M.-J. Sher, X. Wu, M. T. Trinh, A. Fisher, J. Corbett, X.-Y. Zhu, H. I. Karunadasa, A. M. Lindenberg, *J. Phys. Chem. Lett.* 2016, *7*, 2258 – 2263.
[14] K. Thirumal, W. K. Chong, W. Xia, R. Ganguly, S. K. Muduli, M. Sherburne, M. Asta, S. Mhaisalkar, T. C. Sum, H. S. Soo, N. Mathews, *Chem. Mater.* 2017, *29*, 3947 – 3953.
[15] L. Mao, Y. Wu, C. C. Stoumpos, B. Traore, C. Katan, J. Even, M. R. Wasielewski, M. G. Kanatzidis, *J. Am. Chem. Soc.* 2017, *139*, 11956 – 11963.
[16] D. Y. Park, S.-J. An, C. Lee, D. A. Nguyen, K.-N. Lee, M. S. Jeong, *J. Phys. Chem. Lett.* 2019, *10*, 7942 – 7948.
[17] D. Cortecchia, J. Yin, A. Petrozza, C. Soci, *J. Mater. Chem. C* 2019, *7*, 4956 – 4969.
[18] X. Wang, W. Meng, W. Liao, J. Wang, R. G. Xiong, Y. Yan, *J. Phys. Chem. Lett.* 2019, *10*, 501 – 506.
[19] D. Cortecchia, J. Yin, A. Bruno, S.-Z. A. Lo, G. G. Gurzadyan, S. Mhaisalkar, J.-L. Brédas, C. Soci, *J. Mater. Chem. C* 2017, *5*, 2771 – 2780.
[20] J. Yin, H. Li, D. Cortecchia, C. Soci, J.-L. Brédas, *ACS Energy Lett.* 2017, *2*, 417 – 423.
[21] C. Katan, N. Mercier, J. Even, *Chem. Rev.* 2019, *119*, 3140 – 3192.
[22] E. P. Booker, T. H. Thomas, C. Quarti, M. R. Stanton, C. D. Dashwood, A. J. Gillett, J. M. Richter, A. J. Pearson, N. J. L. K. Davis, H. Sirringhaus, M. B. Price, N. C. Greenham, D. Beljonne, S. E. Dutton, F. Deschler, *J. Am. Chem. Soc.* 2017, *139*, 18632 – 18639.
[23] G. M. Paternò, N. Mishra, A. J. Barker, Z. Dang, G. Lanzani, L. Manna, A. Petrozza, *Adv. Funct. Mater.* 2018, *28*, 1805299.
[24] D. Cortecchia, S. Neutzner, A. R. Srimath Kandada, E. Mosconi, D. Meggiolaro, F. De Angelis, C. Soci, A. Petrozza, *J. Am. Chem. Soc.* 2017, *139*, 39 – 42.
[25] K. Z. Du, Q. Tu, X. Zhang, Q. Han, J. Liu, S. Zauscher, D. B. Mitzi, *Inorg. Chem.* 2017, *56*, 9291 – 9302.
[26] Z. Cheng, J. Lin, *CrystEngComm* 2010, *12*, 2646 – 2662.
[27] B. Saparov, D. B. Mitzi, *Chem. Rev.* 2016, *116*, 4558 – 4596.
[28] K. Robinson, G. V. Gibbs, P. H. Ribbe, *Science* 1971, *172*, 567 – 570.
[29] K. Shibuya, M. Koshimizu, F. Nishikido, H. Saito, S. Kishimoto, *Acta Crystallogr. Sect. E* 2009, *65*, m1323 – m1324.
[30] B. Febriansyah, T. M. Koh, Y. Lekina, N. F. Jamaludin, A. Bruno, R. Ganguly, Z. X. Shen, S. G. Mhaisalkar, J. England, *Chem. Mater.* 2019, *31*, 890 – 898.

[31] A. Lemmerer, D. G. Billing, *CrystEngComm* 2010, *12*, 1290 – 1301.
[32] Z. Tang, J. Guan, A. M. Guloy, *J. Mater. Chem.* 2001, *11*, 479 – 482.
[33] X.-N. Li, P.-F. Li, W.-Q. Liao, J.-Z. Ge, D.-H. Wu, H.-Y. Ye, *Eur. J. Inorg. Chem.* 2017, 938 – 942.
[34] J. L. Knutson, J. D. Martin, D. B. Mitzi, *Inorg. Chem.* 2005, *44*, 4699 – 4705.
[35] D. Cortecchia, S. Neutzner, J. Yin, T. Salim, A. R. Srimath Kandada, A. Bruno, Y. M. Lam, J. Martí-Rujas, A. Petrozza, C. Soci, *APL Mater.* 2018, *6*, 114207.
[36] X. Gong, O. Voznyy, A. Jain, W. Liu, R. Sabatini, Z. Piontkowski, G. Walters, G. Bappi, S. Nokhrin, O. Bushuyev, M. Yuan, R. Comin, D. McCamant, S. O. Kelley, E. H. Sargent, *Nat. Mater.* 2018, *17*, 550 – 556.
[37] G. E. Wang, G. Xu, M. S. Wang, L. Z. Cai, W. H. Li, G. C. Guo, *Chem. Sci.* 2015, *6*, 7222 – 7226.
[38] T. Schmidt, K. Lischka, W. Zulehner, *Phys. Rev. B* 1992, *45*, 8989 – 8994.
[39] K. M. McCall, C. C. Stoumpos, S. S. Kostina, M. G. Kanatzidis, B. W. Wessels, *Chem. Mater.* 2017, *29*, 4129 – 4145.
[40] D. Meggiolaro, S. G. Motti, E. Mosconi, A. J. Barker, J. Ball, C. Andrea Riccardo Perini, F. Deschler, A. Petrozza, F. De Angelis, *Energy Environ. Sci.* 2018, *11*, 702 – 713.
[41] L. Martiradonna, *Nat. Mater.* 2018, *17*, 377.
[42] A. D. Martinez, E. L. Warren, P. Gorai, K. A. Borup, D. Kuciauskas, P. C. Dippo, B. R. Ortiz, R. T. Macaluso, S. D. Nguyen, A. L. Greenaway, S. W. Boettcher, A. G. Norman, V. Stevanovic´, E. S. Toberer, A. C. Tamboli, *Energy Environ. Sci.* 2016, *9*, 1031 – 1041.